Imaging the Evolution of Lateral Composition Modulation in Strained Alloy Superlattices

Chris Pearson

Department of Computer Science, Engineering Science, and Physics, The University of Michigan–Flint,
Flint, Michigan 48502, USA

C. Dorin and J. Mirecki Millunchick

Department of Materials Science and Engineering, The University of Michigan, Ann Arbor, Michigan 48109, USA

B. G. Orr

Department of Physics, The University of Michigan, Ann Arbor, Michigan, 48109, USA

Scanning tunneling microscopy is used to investigate the morphological evolution of GaAs/InAs short period superlattice structures. The layers of the superlattice, either grown in compression or tension, exhibit an island or trench morphology. With increasing film thickness, the islands or trenches grow in size and develop a characteristic spacing along [110] of ~150 Å. This is the first experimental evidence to suggest that lateral composition modulation arises from both thickness variations of the layers and compositional nonuniformities within the atomic plane.

There is great interest in the development of novel electronic and photonic devices that utilize one-dimensional confinement of carriers. While many techniques have been employed to create such structures, including advancements in nanolithography [1] and growth on vicinal substrates [2], a promising approach utilizes strain related self-organized growth observed in short period superlattice (SPS) structures [3,4]. Growing strain-balanced SPS structures with appropriate growth parameters can result in spontaneous phase separation during growth creating a film that exhibits carrier confinement. While single-layer films have been extensively studied [5–9], the stability of multilayer films with respect to morphological and compositional variations is not as well understood, and only recently have models been proposed describing these phenomena in strained-layer superlattices [10,11]. One proposal is that thickness variations in a multilayer film create lateral variations in the average composition [10,12]. Local variations of the multilayer composition likely contribute to the phenomenon as well.

Lateral composition modulation (LCM) in SPS structures has been studied using a variety of experimental techniques including atomic force microscopy [13], x-ray diffraction (XRD) [14], and cross-section transmission electron microscopy (TEM) [15]. Cross-section transmission electron micrographs of SPS structures that exhibit LCM show alternating variations in the image contrast, which reflect changes in the composition [15]. High magnification images indicate that the individual superlattice layers undulate in phase with the composition modulation [4]. Once the modulation develops, which typically occurs during the initial ~10 SPS periods, it continues through more than 100 periods [16]. Characteristic modulation wavelengths for GaAs/InAs SPS structures range from 150 to 300 Å, with a composition modulation amplitude of 20% [17]. While much has been learned using TEM and XRD about the growth conditions necessary for LCM to appear [17], an *in situ* technique such as scanning tunneling microscopy (STM) is required in order to study the initiation mechanisms on the evolving surface.

In this Letter, we investigate the growing surface of GaAs/InAs SPS films at several thicknesses for both InAs and GaAs surfaces in order to examine the evolution of the self-organizing process leading to LCM. With increasing SPS thickness, the characteristic features on each surface, islands on the InAs surface and trenches on the GaAs surface, organize with a spacing along [110] of ~150 Å. Different reconstructions observed on the surface suggest that, in addition to thickness variations, compositional variations contribute to the formation of LCM.

Samples were grown in a molecular beam epitaxial chamber using solid sources for In and Ga and a valved cell for As_4. The In and Ga sources were calibrated prior to growth using reflection high-energy electron diffraction (RHEED) intensity oscillations. InP(001) substrates were prepared by heating in an As_4 overpressure [beam equivalent pressure (BEP) $= 12 \times 10^{-6}$ torr] until a change in the surface reconstruction from (2×4) to (4×2) was observed with RHEED, near $T = 540\,°C$. The substrate temperature was then reduced to $T = 480\,°C$ and growth commenced. A 250 nm thick lattice matched $In_{0.53}Ga_{0.47}As$ buffer layer was grown first, followed by the SPS, consisting of 2 ML (monolayer) of GaAs followed by 2 ML of InAs.

An integral period SPS is formed by terminating the growth with InAs, while a fractional period SPS is formed by terminating with GaAs. During growth,

RHEED patterns were (3×2) during deposition of the GaAs layers and an incommensurate (2×3) [18] during the deposition of InAs layers. At the conclusion of growth, samples were cooled quickly $(>1\,°C/s)$ in a reduced As_4 overpressure $(BEP = 6 \times 10^{-6}$ torr) until $T = 300\,°C$ and transferred in ultrahigh vacuum to the STM. Filled state images were acquired for all samples using typically -3 V sample bias and 100 pA of tunneling current.

The InAs-terminated surfaces are covered with a high density of 2D islands as shown in Fig. 1(a). There is a distinct anisotropy observed in the image as the islands and the terraces are composed of rows oriented along $[1\bar{1}0]$. However, the nature of the rows forming the islands and terraces is quite different. The terrace rows meander while the island rows are straight. In Fig. 1(b), a region of the surface is shown in greater detail and the island reconstruction, long rows of bean shaped structures, becomes evident. The separation between the structures along $[1\bar{1}0]$ is approximately 8 Å and the rows are spaced 17 Å apart along [110]. These values together with the characteristic bean shape suggest a $\beta2(2 \times 4)$ reconstruction similar to that observed on the (001) surface of InAs [19] or GaAs [20]. Within the terrace, the rows are spaced approximately 12 Å apart, which corresponds to $3\times$ the underlying bulk lattice spacing along [110]. The terrace reconstruction is consistent with a $(n \times 3)$ reconstruction observed in InGaAs alloys [18,21]. The step height is nearly 3 Å, which is the height of one monolayer, while the $\beta2(2 \times 4)$ island height is roughly 1.5 Å measured with respect to the $(n \times 3)$ terrace. The height difference between the islands and terraces indicates that the islands nucleate on top of the terraces and are associated with local In enrichment of the alloy layer [21].

The surface morphology is quite different when the SPS is terminated with a GaAs layer, as shown in Fig. 2(a). Note that this surface has an additional 2 ML of GaAs as compared to the surface shown in Fig. 1. In contrast to the appearance of the InAs-terminated surface, flat mesas bordered by deep trenches characterize

this surface. The trenches are oriented along $[1\bar{1}0]$ and vary in depth from nearly 3 Å to greater than 15 Å. Again, the surface features are anisotropic as rows are aligned along $[1\bar{1}0]$. In a high resolution image of the surface, shown in Fig. 2(b), it is evident that the mesa comprises several different reconstructions. In one region, a $c(4 \times 4)$ reconstruction displaying the familiar bricklike pattern of surface dimers, similar to an As stabilized GaAs(001) surface [22], is apparent. In an adjacent region, a $(n \times 3)$ reconstruction is again observed. The step height of the mesa is nearly 3 Å and there is no discernible height difference between regions of different reconstructions within the terrace.

The evolution of the growing surface has been investigated by examining SPS structures of several different thickness values. Figures 3(a)–3(c) show a series of images of 5, 10, and 15 periods, respectively. As the thickness of the SPS increases, the 2D islands become longer and the surfaces are nearly devoid of small islands. Also, a characteristic spacing between islands along [110] emerges. The step density increases with increasing SPS thickness, suggesting that there is greater layer instability for thicker structures. A similar series of images of 5.5, 10.5, and 15.5 periods is shown in Figs. 3(d)–3(f), respectively. With increasing SPS thickness, the trenches grow in both areal size and depth, but the overall morphological characteristics of flat mesas bordered by deep trenches are preserved.

A correlation analysis of the images was performed in order to determine whether a lateral correlation exists and to measure the spacing between surface features. For each termination, binary images of the islands (or trenches) with respect to the terraces were created using a threshold technique. An autocorrelation of each image was performed and a line profile of the intensity taken along [110] was recorded. The profiles from several images were averaged together. Results from InAs-terminated samples are shown in Fig. 4(a) and from GaAs-terminated samples in Fig. 4(b). A peak in the correlation profile indicates that there is a positive
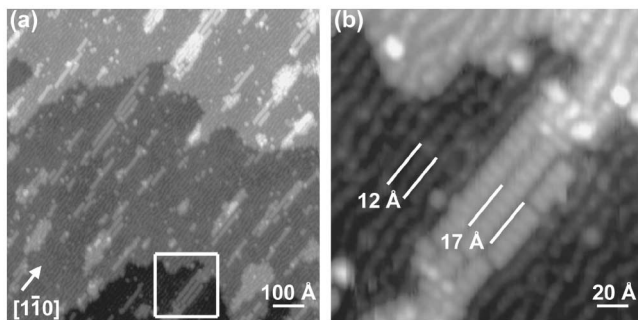
FIG. 1. (a) A 1000 Å $\times$ 1000 Å STM image of a 5 period InAs-terminated SPS. The surface is covered with numerous islands preferentially oriented along $[1\bar{1}0]$. (b) Row spacing of 17 Å for islands and 12 Å for terraces is shown in a 200 Å $\times$ 200 Å high-resolution image.
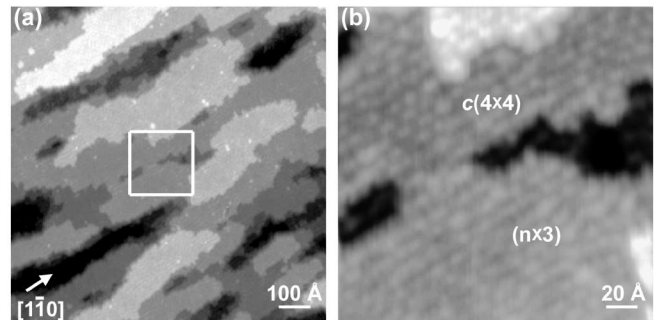
FIG. 2. (a) A 1000 Å $\times$ 1000 Å STM image of a 5.5 period GaAs-terminated SPS. Mesas bordered by deep trenches oriented along $[1\bar{1}0]$ characterize the surface. (b) Regions of $c(4 \times 4)$ and $(n \times 3)$ reconstructions can be discerned in a 200 Å $\times$ 200 Å high-resolution image.
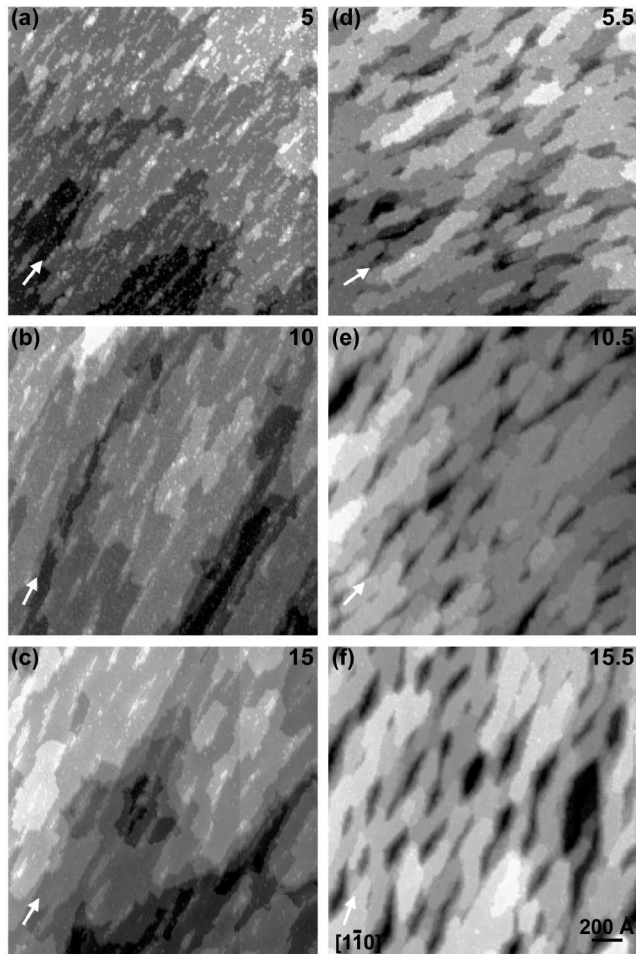
FIG. 3. A sequence of $2000 \, \text{Å} \times 2000 \, \text{Å}$ STM images of InAs-terminated (a)–(c) and GaAs-terminated (d)–(f) SPS. With increasing SPS thickness, the islands (a)–(c) or trenches (d)–(f) grow in size and develop a characteristic spacing along [110]. The arrows indicate the $[1\bar{1}0]$ direction.

FIG. 4. Autocorrelation intensity profiles taken along [110] from InAs-terminated (a) and GaAs-terminated (b) samples show that the surface features, islands (a) and trenches (b), develop a characteristic spacing of $\sim 150 \, \text{Å}$.

probability of finding a similar surface feature when traversing the sample along [110]. A common characteristic for each profile is a peak located $\sim 150 \, \text{Å}$ away from the central peak, indicating that there is a characteristic island-island or trench-trench spacing of $\sim 150 \, \text{Å}$ along [110]. InAs-terminated samples show a single peak for the thinnest samples with a second peak, which indicates a higher degree of correlation, developing as the SPS becomes thicker. The GaAs-terminated samples show two peaks indicating that the trench spacing is well ordered even in the thinnest samples. The peak spacing ranges between ~ 150 and $\sim 170 \, \text{Å}$, which is similar to the compositional modulation wavelength observed with TEM for thicker samples of this material system at these growth conditions [17].

The island or trench morphology observed for the InAs- and GaAs-terminated surfaces is a consequence of the sign of the strain of each layer in the superlattice. The free energy of the system governs the formation of steps and the subsequent morphology. If the energy

gained from the strain relaxation of a step edge is larger than the energy required to create a step, the surface will roughen [23]. It is well known that the step energy depends upon the sign of the strain [24]. Additionally, it has been demonstrated that the step curvature is also influenced by the sign of the strain [25]. Compressive strain favors convex steps leading to an islanded morphology, while tensile strain favors concave steps leading to a trench or pitted morphology. This is consistent with our results, which show that the morphology is characterized by islands on the InAs (compressive) layers, as seen in Fig. 1(a), and trenches on the GaAs (tensile) layers, as seen in Fig. 2(a).

Lateral composition modulation in these structures [26] can arise from two different mechanisms: (1) no intermixing of the individual superlattice layers with variations in layer thickness or (2) nonuniform intermixing of planar layers. When there is no intermixing, the individual superlattice layers remain pure GaAs and pure InAs, but the thickness of the layers varies resulting in an average LCM. Thickness variations in these 2 ML thick layers are not observed in cross-section TEM because they are not coherent through the thickness of the foil. The island-island and trench-trench correlations shown

in Fig. 4 are nominally equivalent to each other and are also nearly the same as the modulation wavelength observed by TEM consistent with mechanism (1)—no intermixing.

Since the GaAs-terminated samples show two peaks in the correlation profile even for the thinnest samples [Fig. 4(b)] it is likely that the initial GaAs (tensile) layer creates the template for subsequent layers. When the InAs (compressive) layer is grown on top, the larger In atoms preferentially grow within the trenches, which are regions of the surface that have been partially strain relieved [5]. As the growth of the compressive layer continues, islands nucleate on the regions of partial strain relief. When the ensuing GaAs layer is grown, the smaller Ga atoms avoid the islands due to strain, and create mesas between the islands [27]. In this manner, thickness variations develop. While topographical images alone cannot conclusively establish if islands grow within trenches and mesas between islands, previous results show that Ge quantum dots with Si spacers [28] and InAs quantum dots with GaAs spacers [27] become vertically aligned due to the interaction of strain fields of the buried dots with the growing film. This description is also consistent with the linear stability model of Shilkrot et al. [10], which shows that an initial instability on the surface may propagate through an entire multilayer.

In the other mechanism for LCM, the layers are uniformly thick, but the components intermix nonuniformly, resulting in composition variations within the plane of the film. As shown in Figs. 1(b) and 2(b) there are several surface reconstructions observed in different regions of the sample, suggesting that the local composition varies within the atomic plane. It is well known that In surface segregation causes intermixing of the layers [29]. The LCM in these structures is therefore a result of both thickness variations of the individual layers and compositional variations within each layer. This is especially clear for the InAs-terminated surfaces on which the 2D islands possess a lateral correlation consistent with the modulation wavelength and also have reconstructions associated with high In content [21].

The different reconstructions observed on the surface arise from real variations in the composition that exist during growth and are not an artifact of the cooling process. In order to demonstrate this, imaged samples were returned to the growth chamber and annealed to $T = 350\,°C$ for ~5 min under only a residual As$_4$ overpressure. Annealing did not significantly change the surface as the step and island structure was retained, as was the overall distribution of surface reconstructions.

In summary, we have used *in situ* STM to image the growing surface of both InAs- and GaAs-terminated SPS structures with various thicknesses. Each surface displays a markedly different morphology. The GaAs-terminated surface is characterized by flat mesas bordered by deep trenches and the InAs-terminated surface is decorated with islands. The islands or trenches show a regular separation along [110] and autocorrelation intensity profiles along this direction show an island-island or trench-trench spacing of ~150 Å. This result suggests that LCM is initiated by the vertical stacking of 2D islands and trenches and is enhanced by variations of the composition within the atomic plane, as evidenced by different surface reconstructions.

[1] Joon Hyung Bae, Takahito Ono, and Masayoshi Esashi, Appl. Phys. Lett. **82**, 814 (2003).
[2] Jong-Su Lee et al., J. Cryst. Growth **249**, 201 (2003).
[3] K. Y. Chen, K. C. Hsieh, and J. N. Baillargeon, Appl. Phys. Lett. **60**, 2892 (1992).
[4] J. Mirecki Millunchick et al., Appl. Phys. Lett. **70**, 1402 (1997).
[5] J. E. Guyer, S. A. Barnett, and P. W. Voorhees, J. Cryst. Growth **217**, 1 (2000).
[6] B. J. Spencer, P. W. Voorhees, and J. Tersoff, Phys. Rev. B **64**, 235318 (2001).
[7] Frank Glas, Phys. Rev. B **55**, 11 277 (1997).
[8] I. P. Ipatova et al., Phys. Rev. B **57**, 12 968 (1998).
[9] François Léonard and Rashmi C. Desai, Appl. Phys. Lett. **74**, 40 (1999).
[10] L. E. Shilkrot, D. J. Srolovitz, and J. Tersoff, Phys. Rev. B **62**, 8397 (2000).
[11] Zhi-Feng Huang and Rashmi C. Desai, Phys. Rev. B **67**, 075416 (2003).
[12] D. W. Stokes et al., J. Appl. Phys. **93**, 311 (2003).
[13] A. G. Norman et al., Appl. Phys. Lett. **73**, 1844 (1998).
[14] J. H. Li et al., Phys. Rev. B **66**, 115312 (2002).
[15] R. D. Twesten et al., Phys. Rev. B **60**, 13 619 (1999).
[16] S. P. Ahrenkiel et al., J. Appl. Phys. **84**, 6088 (1998).
[17] C. Dorin and J. Mirecki Millunchick, J. Appl. Phys. **91**, 237 (2002).
[18] J. G. Belk et al., Surf. Sci. **387**, 213 (1997).
[19] W. Barvosa-Carter et al., Surf. Sci. **499**, L129 (2002).
[20] V. P. LaBella et al., Phys. Rev. Lett. **83**, 2989 (1999).
[21] J. Mirecki Millunchick et al., Appl. Phys. Lett. **83**, 1361 (2003).
[22] Akihiro Ohtake, Phys. Rev. Lett. **89**, 206102 (2002).
[23] J. Tersoff, Appl. Surf. Sci. **102**, 1 (1996).
[24] Y. H. Xie et al., Phys. Rev. Lett. **73**, 3006 (1994).
[25] P. Krapf et al., Phys. Rev. B **55**, R10 229 (1997).
[26] For a schematic of the structure in question, please refer to Fig. 1 in Ref. [15].
[27] Qianghua Xie et al., J. Cryst. Growth **150**, 357 (1995).
[28] J. Tersoff, C. Teichert, and M. G. Lagally, Phys. Rev. Lett. **76**, 1675 (1996).
[29] J. M. Moison et al., Phys. Rev. B **40**, 6149 (1989).